EXTENDED PDF FORMAT
SPONSORED BY

BIO-RAD

http://discover.bio-rad.com



Ice Core Records of Atmospheric N2O Covering the Last 106,000 Years

Todd Sowers, *et al.*

Science **301**, 945 (2003);
DOI: 10.1126/science.1085293

The following resources related to this article are available online at www.sciencemag.org (this information is current as of December 29, 2006):

Updated information and services, including high-resolution figures, can be found in the online version of this article at:
http://www.sciencemag.org/cgi/content/full/301/5635/945

Supporting Online Material can be found at:
http://www.sciencemag.org/cgi/content/full/301/5635/945/DC1

This article **cites 8 articles**, 3 of which can be accessed for free:
http://www.sciencemag.org/cgi/content/full/301/5635/945#otherarticles

This article has been **cited by** 14 article(s) on the ISI Web of Science.

This article has been **cited by** 1 articles hosted by HighWire Press; see:
http://www.sciencemag.org/cgi/content/full/301/5635/945#otherarticles

This article appears in the following **subject collections**:
Atmospheric Science
http://www.sciencemag.org/cgi/collection/atmos

Information about obtaining **reprints** of this article or about obtaining **permission to reproduce this article** in whole or in part can be found at:
http://www.sciencemag.org/help/about/permissions.dtl

Downloaded from www.sciencemag.org on December 29, 2006

Science (print ISSN 0036-8075; online ISSN 1095-9203) is published weekly, except the last week in December, by the American Association for the Advancement of Science, 1200 New York Avenue NW, Washington, DC 20005. Copyright c 2006 by the American Association for the Advancement of Science; all rights reserved. The title SCIENCE is a registered trademark of AAAS.

MV/cm are shown. The change of R_{Hall} as a function of time, t, is displayed in Fig. 3A. Because the magnitude of $\mu_0 H_0 = -0.2$ mT is smaller than the coercive force $\mu_0 H_C = -0.5$ mT under $E = -1.5$ MV/cm, the state remains at point A until we switch E to 0 at $t = 25$ s. There is an absence of relaxation in this 25-s period, which indicates that the state is stable. In response to the switching, the sign of R_{Hall} changes from positive to negative, showing that electrical switching triggers magnetization reversal. Because $|H_C| < |H_0|$ at $E = 0$ V/cm, the electrical switching brings the state to point B of the inset. Once the magnetization is reversed, the sign of R_{Hall} and thus M remains negative and shows only a small variation when E is switched back and forth between 0 and -1.5 MV/cm, as shown by region C and region D (corresponding to point C and D in the inset, respectively). This electrically assisted magnetization reversal ("assisted" because a small negative magnetic field is needed) without changing applied magnetic fields or temperature demonstrates the possibility of a new scheme for Curie point writing, where magnetization reversal is assisted by making the system closer to or making it go beyond its Curie temperature (*12*).

At a higher temperature range, one expects to be able to completely demagnetize the material solely by applying an external electric field without resorting to conventional techniques such as increasing temperature or using oscillating magnetic fields. With sample B at 33 K (Fig. 3B), the $R_{Hall} - \mu_0 H$ hysteresis loop shown in closed triangles under $E = -1.5$ MV/cm is measured. Then E is set to $+1.5$ MV/cm, which makes the $R_{Hall} - \mu_0 H$ curve a linear one with no hysteresis (closed circles). Switching back E to -1.5 MV/cm, one can obtain an initial curve (i.e., a virgin curve; open triangles), demonstrating an isothermal demagnetization of a ferromagnetic material. The initial magnetization curve suggests that domain nucleation is responsible for the magnetization reversal in (In,Mn)As, as opposed to domain pinning, because the magnetization of the initial curve reaches saturation at a magnetic field much smaller than the coercive field in the hysteresis loop (*13*). We expect that well-developed magnetic domains similar to the one in a ferromagnetic semiconductor such as (Ga,Mn)As (*14*–*16*) are present in (In,Mn)As as a result of the long-range nature of carrier-mediated ferromagnetic interaction, even though (In,Mn)As is a dilute magnetic alloy.

Because electrical manipulation of magnetization processes presented here offers functionalities not previously accessible, ferromagnetic semiconductors are expected to play a key role in magnetoelectronics and spintronics (*17*, *18*) once their T_C reaches well beyond room temperature. The highest T_C reported for (In,Mn)As and (Ga,Mn)As (*19*) in its thin-film form is 60 K ($x = 0.063$) (*20*) and 160 K ($x = 0.074$) (*21*), respectively, which is well accounted for by the Zener model of carrier-induced ferromagnetism (*9*, *10*). Because theoretical prediction by the same model shows that T_C increases linearly with Mn concentration and $p^{1/3}$ with hole density, an increase of Mn concentration by a factor of 5 for (In,Mn)As and a factor of 2 for (Ga,Mn)As, without reducing hole concentration, should allow T_C to go beyond room temperature. This has not yet been realized experimentally; such a possibility has been hampered so far by the formation of NiAs-type MnAs as a second phase that reduces the Mn concentration in the host and/or by the formation of Mn interstitials (a double donor) that reduce the hole concentration (*22*–*24*). Other material systems like GaN and ZnO are predicted to show promise in realizing room-temperature carrier-induced ferromagnetism if the physics demonstrated for the model holds for these materials (*9*, *10*).

References and Notes

1. J. Slonczewski, *J. Magn. Magn. Mater.* **159**, L1 (1996).
2. L. Berger, *Phys. Rev. B* **54**, 9353 (1996).
3. M. Tsoi *et al.*, *Phys. Rev. Lett.* **80**, 4281 (1998).
4. E. B. Myers, D. C. Ralph, J. A. Katine, R. N. Louie, R. A. Buhrman, *Science* **285**, 867 (1999).
5. F. J. Albert, J. A. Katine, R. A. Buhrman, D. C. Ralph, *Appl. Phys. Lett.* **77**, 3809 (2000).
6. H. Ohno, H. Munekata, T. Penny, S. von Molnár, L. L. Chang, *Phys. Rev. Lett.* **68**, 2664 (1992).
7. H. Ohno *et al.*, *Nature* **408**, 944 (2000).
8. H. Munekata, A. Zaslavsky, P. Fumagalli, R. J. Gambino, *Appl. Phys. Lett.* **63**, 2929 (1993).
9. T. Dietl, H. Ohno, F. Matsukura, J. Cibert, D. Ferrand, *Science* **287**, 1019 (2000).
10. T. Dietl, H. Ohno, F. Matsukuta, *Phys. Rev. B* **63**, 195205 (2001).
11. Sample structure and properties are available as supporting material on *Science* Online.
12. Curie point writing is being used in magneto-optical memory disks and is currently being investigated for ultrahigh-density magnetic recording. In both cases, it is done by heating the region of interest using laser-light irradiation.
13. G. Bertotti, *Hysteresis in Magnetism* (Academic Press, San Diego, CA, 1998), chap. 10.
14. T. Shono, T. Hasegawa, T. Fukumura, F. Matsukura, H. Ohno, *Appl. Phys. Lett.* **77**, 1363 (2000).
15. U. Welp, V. K. Vlasko-Vlasov, X. Liu, J. K. Furdyna, T. Wojtowicz, *Phys. Rev. Lett.* **90**, 167206 (2003).
16. T. Dietl, J. König, A. H. MacDonald, *Phys. Rev. B* **64**, 241201 (2001)
17. H. Ohno, F. Matsukura, Y. Ohno, *JSAP Int.* **5**, 4 (2002); available at www.jsapi.jsap.or.jp/.
18. S. A. Wolf *et al.*, *Science* **294**, 1488 (2001).
19. H. Ohno, *Science* **281**, 951 (1998).
20. D. Chiba, unpublished work, see also H. Ohno, *J. Cryst. Growth* **251**, 285 (2003).
21. D. Chiba, K. Takamura, F. Matsukura, H. Ohno, *Appl. Phys. Lett.* **82**, 3020 (2003).
22. K. M. Yu *et al.*, *Phys. Rev. B* **65**, 201303 (2002).
23. F. Máca, J. Mašek, *Phys. Rev. B* **65**, 235209 (2002).
24. S. C. Erwin, A. G. Petukov, *Phys. Rev. Lett.* **89**, 227201 (2002).

25. We thank K. Takanashi, S. Mitani, T. Dietl, M. Shirai, K. Ohtani, and Y. Ohno for useful discussions. This work was partially supported by the IT Program of RR2002 from the Ministry of Education, Culture, Sports, Science and Technology of Japan, Grant-in-Aids and a Research Fellowship from the Japan Society for the Promotion of Science, and the Sasakawa Scientific Research Grant from the Japan Scientific Society.

Supporting Online Material
www.sciencemag.org/cgi/content/full/1086608/DC1
SOM Text
Fig. S1

8 May 2003; accepted 26 June 2003
Published online 10 July 2003;
10.1126/science.1086608
Include this information when citing this paper.

Downloaded from www.sciencemag.org on December 29, 2006

Ice Core Records of Atmospheric N_2O Covering the Last 106,000 Years

Todd Sowers,* Richard B. Alley, Jennifer Jubenville

Paleoatmospheric records of trace-gas concentrations recovered from ice cores provide important sources of information on many biogeochemical cycles involving carbon, nitrogen, and oxygen. Here, we present a 106,000-year record of atmospheric nitrous oxide (N_2O) along with corresponding isotopic records spanning the last 30,000 years, which together suggest minimal changes in the ratio of marine to terrestrial N_2O production. During the last glacial termination, both marine and oceanic N_2O emissions increased by 40 ± 8%. We speculate that our records do not support those hypotheses that invoke enhanced export production to explain low carbon dioxide values during glacial periods.

Nitrous oxide (N_2O) is an important component of the atmosphere that behaves as a "greenhouse" gas and participates in many atmospheric chemical reactions involving O_3, NO_y, and OH. Tropospheric N_2O levels are controlled by bacterial N_2O emissions from the terrestrial and marine biospheres, stratospheric photolysis and photooxidation of N_2O, and the stratosphere-troposphere air exchange rate (*1*, *2*).

During the last glacial-interglacial transition, atmospheric N_2O values increased from ~190 to 265 parts per billion (ppb) (*3*–*5*). Model studies suggest that the lifetime of N_2O in the atmosphere has remained effectively constant over the last 18,000 years (18

ky) (*6*, *7*). This implies that the observed N_2O concentration ([N_2O]) variations have been the result of changes in the source strength. N_2O oscillations have been documented during the cold Younger Dryas event and the one Dansgaard/Oeschger (D/O) event (number 8) that has been studied in detail. These events also have large documented fluctuations in atmospheric methane (CH_4) concentration that are likely the result of changes in CH_4 emissions from terrestrial wetlands. Wetland CH_4 emissions increase with temperature, primary productivity, and soil saturation (*8*–*10*). Terrestrial N_2O emissions behave similarly, but are highest for soils with between 60 and 90% water-filled pore spaces; at higher saturation, the low-redox conditions promote complete reduction of NO_3^- to N_2 gas, whereas in drier areas NO emissions dominate (*11*, *12*).

Department of Geosciences and the EMS Environment Institute, Pennsylvania State University, University Park, PA 16802, USA.

*To whom correspondence should be addressed. E-mail: sowers@geosc.psu.edu

Here, we extend the ice core N_2O record back to 106,000 years ago (106 ka) and provide atmospheric N_2O isotope results spanning the last glacial termination. Concentration measurements were made on 106 samples of Greenland Ice Sheet Project 2 (GISP II), central Greenland (73°N, 38°W), ice with gas ages ranging from 0.5 to 106 ka (*10*) by means of a dry extraction technique (*13*, *14*). Samples integrating fewer than 30 years of atmospheric history are spaced on average 1.1 ky apart. The overall external precision and blank associated with the technique are ±5 and 4 ± 4 ppb, respectively (1σ errors). In addition, we measured 24 samples of ice from the Taylor Dome, Antarctica, ice core (77°47′S, 158° 43′E) for [N_2O], $\delta^{15}N$, and $\delta^{18}O$ of N_2O using a previously described technique (*15*). The external precision for the $\delta^{15}N$ and $\delta^{18}O$ measurements is ±0.5‰ and ±2‰, respectively, based on six samples of ice with gas ages between 1785 and 1820 A.D. (1σ errors). The ages of the Taylor Dome samples were previously determined by correlating the CH_4 record from Taylor Dome into the GISP II record (*16*). All data (concentration and isotopic) have been corrected for all mass-dependent fractionation processes (including gravitational fractionation) based on $\delta^{15}N$ of N_2 data that were measured on each gas sample (*17*, *18*).

The N_2O concentration data from the GISP II and Greenland Ice Core Project (GRIP), Greenland, and Dome C, Antarctica, cores are plotted in Fig. 1 (*3*). The ages for GRIP N_2O data have been transferred to the GISP II time scale for direct comparison (*19*). The N_2O data sets were generated with different extraction techniques that yield very similar N_2O records during overlapping periods, suggesting that, in general, the ice core records are likely to reflect paleoatmospheric N_2O fluctuations within experimental uncertainty. There are two major exceptions. First, the N_2O values from GISP II are low in the depth interval where air bubbles are transformed to solid clathrates [900 to 1400 m, gas ages of 4 to 8 ka (*20*)]. These results are readily explained by preferential incorporation of N_2O into, but incomplete gas recovery from, the solid air-hydrate phase [supporting online material (SOM) text]. Second, a few N_2O results from the GRIP core (11.8 and 38.9 ka) are anomalously high relative to results from neighboring samples (*3*). These high values are thought to be related to an unidentified artifact that may involve in situ N_2O that was liberated by microbial processes (*15*).

In the lower portion of Fig. 1 we plot the CO_2 records from the Taylor Dome and Vostok ice cores to complete the picture of changes in the concentration of major long-lived bioactive trace-gas species over the last 106 ky (*21*–*23*). We have used a Vostok gas chronology that had previously been tied to the GISP II gas chronology (*24*). Presently, the N_2O record is of lower resolution than either the CH_4 or the $\delta^{18}O_{ice}$ records; for comparison, we have resampled the CH_4, CO_2, and $\delta^{18}O_{ice}$ records at times for which we have N_2O data. The resampled curves are shown with solid lines in Fig. 1.

In Fig. 2 we present results from 21 measurements of the $\delta^{15}N$ and $\delta^{18}O$ of N_2O from the Taylor Dome ice core between 2.6 and 32.6 ka covering the last glacial termination and the Holocene. Unexpectedly, the isotope data show little variability over this period of rapid concentration change, despite the large differences in the characteristic isotope values for the marine and terrestrial N_2O [$\delta^{15}N$ values ~8 ± 3‰ and −15 ± 15‰, $\delta^{18}O$ values ~45 ± 3‰ and 35 ± 15‰ (standard mean ocean water, SMOW) for marine and terrestrial sources, respectively] (*25*). The average $\delta^{15}N$ and $\delta^{18}O$ values from Taylor Dome over the last 33 ky are 11.1 ± 0.8‰ and 46.5 ± 1.7‰, respectively. These aver-

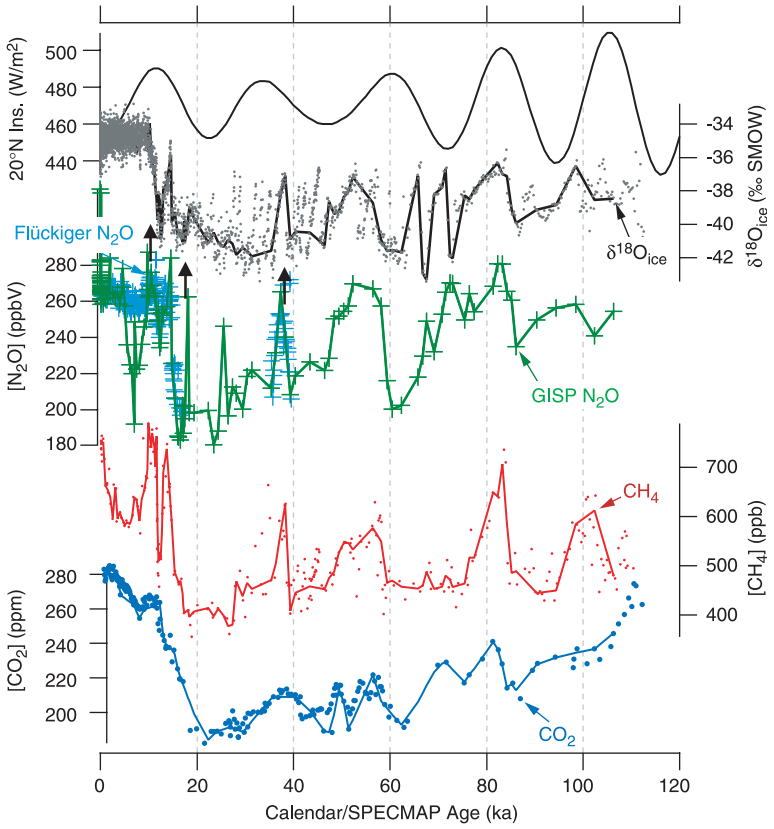


Fig. 1. Various climate records covering the later portion of the last glacial period. Top curve (black): June insolation for 20°N (*44*). The isotopic temperature record for Greenland is shown with gray symbols, with the resampled record denoted by the solid black line (*45*); the green curve is the N_2O record from GISP II, with blue crosses representing N_2O data from Dome C and GRIP (*3*, *4*); the red curve is the resampled CH_4 record from GISP II, with red symbols representing the original record (*10*); and the blue curve is the resampled CO_2 record (*46*) based on the Bender *et al.* Vostok gas age model (*24*). Also included are the CO_2 data (filled blue circles) covering the last 60 ky from the Taylor Dome ice core (*21*–*23*). The three vertical black arrows above the N_2O data represent anomalously high N_2O data obtained from the GRIP core (*3*).

Downloaded from www.sciencemag.org on December 29, 2006

age values are statistically indistinguishable from the preanthropogenic (1785 to 1819 A.D.) values obtained from the GISP II core (10.1 ± 0.6‰ and 47.4 ± 1‰, number of samples n = 6) and Eemian (115 to 130 ka) values from the Vostok core (10.1 ± 1.0‰ and 45.8 ± 0.8‰, n = 5) (*15*, *26*).

The data sets in Figs. 1 and 2 can be used to test models of global biogeochemical cycles involving N_2O across a variety of time scales. With one exception (the Younger Dryas), we suggest that throughout the last 33 ky the ratio of terrestrial to marine N_2O emissions (T/M_{N_2O}) has remained fairly constant. We obviously cannot exclude the possibility that there were substantial changes in T/M_{N_2O} that were offset by tightly coupled changes in the characteristic isotope ratios of the sources and/or sinks that resulted in the nearly constant atmospheric values. However, a more parsimonious explanation would be that marine and terrestrial N_2O emissions have varied together, as suggested by a recent modeling study of the marine N_2O emissions during the Younger Dryas period (*27*).

We can place an upper limit on T/M_{N_2O} variability based on the variability of the N_2O isotope measurements. Under steady conditions, the isotopic composition of atmospheric N_2O is dictated by the fraction of each source or sink multiplied by the characteristic isotope value. Assuming that the primary sink (stratospheric photolysis), its characteristic isotopic effect, and the isotopic values of the sources have remained constant, we can calculate the maximum change in T/M_{N_2O} that is consistent with our measurements. The variability of all $\delta^{15}N$ and $\delta^{18}O$ values about the mean (±0.8‰ and 1.7‰, respectively) is similar to our external analytical precision [±0.5‰ and ±2‰ (*15*)]. This implies that the calculated change in T/M_{N_2O} based on the measured isotope variability is likely to be larger than the true variability. The $\delta^{15}N$ data are more precise and therefore provide the stronger constraint, indicating that T/M_{N_2O} varied by less than 16% throughout the last 33 ky.

Model studies designed to simulate changes in the chemistry of the atmosphere during the last glacial period suggest that the primary sink for N_2O has remained effectively constant (±15%) over the last 18 ky (*6*, *7*). Assuming that the lifetime of N_2O has remained constant (118 years), we can quantitatively assign changes in global sources based on the measured concentration changes. N_2O levels during the LGM were ~190 ppb, implying that global sources were 7.7 Tg N/year. N_2O levels increased during the termination to ~265 ppb because of a 40% (190 to 265 ppb) increase in global N_2O sources. We can then use the $\delta^{15}N$ values to calculate the magnitude of the change in marine and terrestrial N_2O sources during the termination. Using $\delta^{15}N$ values for terrestrial and oceanic N_2O of −15 and 8‰, respectively, and the isotope effect associated with stratospheric photolysis of 1.023 (*26*), we calculate that LGM terrestrial and oceanic N_2O emissions were 4.3 and 3.4 Tg N/year, respectively. Considering the concentration and isotope data together, we conclude that both terrestrial and oceanic N_2O emissions increased by 40 ± 8% during the last termination, accounting for the 40% increase in tropospheric N_2O loading.

Detailed inspection of the isotope results during the Younger Dryas interval (13 to 11.5 ka) suggests that the $\delta^{15}N$ and $\delta^{18}O$ values decreased, as one moves forward in time between 12.4 and 11.4 ka, by 1.8 and 5‰, respectively. This interval covers the end of the Younger Dryas period when atmospheric N_2O values increased by ~20 ppb. Although the measured isotope shift over this interval approximates our uncertainty envelope, the decrease in both $\delta^{15}N$ and $\delta^{18}O$ values over the same interval implies that the trends are probably significant. We believe that these anomalies may be related to enhanced terrestrial N_2O emissions (relative to marine emissions) near the end of the Younger Dryas. This agrees with and strengthens the model results of Goldstein *et al.* (*27*), which require a large increase in terrestrial emissions to explain the concentration change at the end of the Younger Dryas.

Figure 1 shows much shared variance among the disparate indicators [correlation coefficients (r^2) are greater than 0.6 and significantly different from zero between all pairs among N_2O, CH_4, CO_2, and $\delta^{18}O_{ice}$]. Because CO_2 is primarily controlled by marine processes (on millennial time scales), CH_4 by terrestrial processes, N_2O by both terrestrial and marine processes, and $\delta^{18}O_{ice}$ can be viewed as a circum–North Atlantic climate record, the similarities and differences raise numerous fundamental questions about the climate system and the biogeochemical systems that cycle trace-gas species. We focus here on three questions.

First, the significant covariation between CO_2 and N_2O, and the covariation between marine and terrestrial sources of N_2O over the last 30 ky, may provide new insights into the origin of the glacial-interglacial CO_2 variations. Surface-water N_2O levels are generally controlled by N mineralization in the waters above the thermocline, as reflected in the positive correlation between $[N_2O]$ and apparent oxygen utilization (AOU) in the modern ocean (*28*). If the positive N_2O-AOU relation observed today applies for the glacial ocean, then lowering of the surface-water partial pressure of CO_2 (pCO_2) during the LGM through enhanced export production would have promoted elevated oceanic N_2O levels that are not supported by our data. Our data are consistent with those scenarios that predict lowered pCO_2 levels resulting from higher alkalinity, increased stratification, or both (*29*), *30*).

Second, lowered oceanic N_2O emissions during the LGM may reflect decreased emissions from the continental shelves when sea levels were much lower. Present-day estimates of global N_2O emissions from continental shelves range from 0.6 to 2.7 Tg N/year (*31*, *32*). These estimates are comparable to the additional oceanic N_2O emissions that are required to satisfy our concentration and isotope records (1.4 Tg N/year).

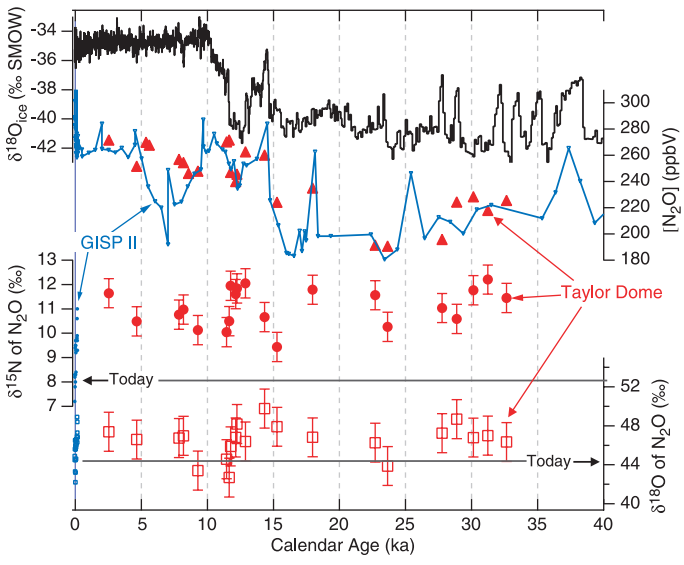


Fig. 2. Measurements of $[N_2O]$ and $\delta^{15}N$ and $\delta^{18}O$ of N_2O from the Taylor Dome ice core are shown in red with 1σ error bars (except $[N_2O]$). Also included are recent isotope data from a shallow core from the GISP II site (*26*) representing the anthropogenic perturbation over the past two centuries. The GISP II $[N_2O]$ data from Fig. 1 are reproduced here in blue for comparison with the Taylor Dome $[N_2O]$ data. Shown for reference (top) is the isotopic temperature record from GISP II, likely representing the mean climate state of the circum–North Atlantic region. Note the small amount of variance in the Taylor Dome isotope data before the anthropogenic era. Present-day $\delta^{15}N$ and $\delta^{18}O$ of N_2O values (8.2 and 44.5‰) are indicated with horizontal lines for reference.

Downloaded from www.sciencemag.org on December 29, 2006

Figure 1 shows that CH_4 and N_2O varied together not only on orbital time scales (the clear precessional signal and slower variations), but also on millennial time scales during the Younger Dryas, Dansgaard/Oeschger interstadial 8, and other events between about 40 and 90 ka. This observation is consistent with monsoonal coupling of terrestrial and marine realms. During periods of increased monsoonal activity (interstadial periods), enhanced upwelling of nutrient-rich water in the Arabian Sea and the Eastern Tropical Pacific supported increased marine productivity and thus increased organic-matter rain. The enhanced flux of organic matter caused a reduction in mid-water oxygen concentration, thereby increasing denitrification; a consequent increase in N_2O production ultimately led to increased N_2O emissions in upwelling areas modulated by monsoonal circulation patterns (*33, 34*). At the same time, enhanced monsoonal rainfall would have expanded the region of wet soils producing CH_4 and N_2O.

One notable exception to the general CH_4/N_2O correspondence occurs during the cooling event that began about 80 ka. N_2O levels remained high for ~7 ky after CH_4 levels dropped precipitously. Perhaps during this period, the CH_4/N_2O temporal relation may reflect greater initial sensitivity of CH_4 emissions to terrestrial drying. Complete soil saturation optimizes CH_4 production, whereas reduced N_2O emissions from drying of some regions below the 60 to 90% saturated window for optimal N_2O production are partially offset by drying of wetter areas into the optimum N_2O emission window. Additionally, because high northern latitudes were more important for CH_4 [~18% of preanthropogenic CH_4 emissions in latitude bands north of 40°N (*8*)] than for N_2O [~9% (*35*)], ice-sheet advance may have impacted CH_4 emissions more directly and quickly than N_2O emissions. Additional isotopic analyses on samples before 30 ka might clarify the relative roles of marine and terrestrial sources of N_2O in these cases, and why this behavior is not shown strongly at other times.

References and Notes

1. Current N_2O emissions from the terrestrial biosphere are estimated to be 12 ± 3 Tg N/year, and preanthropogenic estimates are ~7 Tg N/year (*12*, *36*-*39*). Marine N_2O emissions are estimated to be 4 ± 2 Tg N/year (*40, 41*). About 98% of the total atmospheric N_2O sink occurs in the stratosphere. Minschwaner *et al.* (*42*) estimated the 1980 value to be 12 ± 4 Tg N/year, corresponding to a mean atmospheric lifetime of 118 ± 25 years (*43*).
2. J. R. Holton *et al.*, *Rev. Geophys.* **33**, 403 (1995).
3. J. Fluckiger *et al.*, *Science* **285**, 227 (1999).
4. J. Fluckiger *et al.*, *Global Biogeochem. Cycles* **16**, 1010, doi:10.1029/2001GB001417 (2002).
5. M. Leuenberger, U. Siegenthaler, *Nature* **360**, 449 (1992).
6. P. Martinerie, G. P. Brasseur, C. Granier, *J. Geophys. Res.* **100**, 14291 (1995).
7. P. Crutzen, C. Bruhl, *Geophys. Res. Lett.* **20**, 1047 (1993).
8. J. A. Chappellaz, I. Y. Fung, A. M. Thompson, *Tellus* **45B**, 228 (1993).
9. J. Chappellaz *et al.*, *Nature* **366**, 443 (1993).
10. E. Brook, T. Sowers, J. Orchardo, *Science* **273**, 1087 (1996).
11. A. F. Bouwman, I. Fung, E. Matthews, J. John, *Global Biogeochem. Cycles* **7**, 557 (1993).
12. E. A. Davidson, in *Biogeochemistry and Global Change, Radiatively Active Trace Gases* R. S. Oremland, Ed. (Champman & Hall, New York, 1993), pp. 369–386.
13. J. Jubenville, thesis, Pennsylvania State University (2000).
14. T. A. Sowers, J. Jubenville, *J. Geophys. Res.* **105**, 29155 (2000).
15. T. Sowers, *J. Geophys. Res.* **106**, 31903 (2001).
16. E. J. Brook, S. Harder, J. Severinghaus, E. Steig, C. Sucher, *Global Biogeochem. Cycles* **14**, 559 (2000).
17. T. A. Sowers, M. L. Bender, D. Raynaud, *J. Geophys. Res.* **94**, 5137 (1989).
18. C. M. Trudinger *et al.*, *J. Geophys. Res.* **102**, 6747 (1997).
19. T. Blunier, E. Brook, *Science* **291**, 109 (2001).
20. A. J. Gow *et al.*, *J. Geophys. Res.* **102**, 26559 (1997).
21. A. Indermuhle, E. Monnin, B. Stauffer, T. Stocker, M. Wahlen, *Geophys. Res. Lett.* **27**, 735 (2000).
22. A. Indermuhle *et al.*, *Nature* **398**, 121 (1999).
23. H. J. Smith, H. Fischer, M. Wahlen, D. Mastroianni, B. Deck, *Science* **400**, 248 (1999).
24. M. L. Bender, B. Malize, J. Orchardo, T. Sowers, J. Jouzel, in *Mechanisms of Global Climate Change at Millennial Time Scales*, P. U. Clark, R. S. Webb, L. D. Keigwin, Eds. (American Geophysical Union, Washington, DC, 2000), American Geophysical Union Monograph 112, pp. 149–165.
25. T. Rahn, M. Wahlen, *Global Biogeochem. Cycles* **14**, 537 (2000).
26. T. Sowers, A. Rodebaugh, N. Yoshida, S. Toyoda, *Global Biogeochem. Cycles* **16**, 1129, doi:1029/2002GB001911 (2002).
27. B. Goldstein, F. Joos, T. Stocker, *Geophys. Res. Lett.* **30**, 1092, doi:10.1029/2002GL016418 (2003).
28. J. H. Butler, J. W. Elkins, T. M. Thompson, D. B. Egan, *J. Geophys. Res.* **94**, 14865 (1989).
29. D. M. Sigman, E. A. Boyle, *Nature* **407**, 859 (2000).
30. D. Archer, A. Winguth, D. Lea, N. Mahowald, *Rev. Geophys.* **38**, 159 (2000).
31. S. P. Seitzinger, C. Kroeze, *Global Biogeochem. Cycles* **12**, 93 (1998).
32. H. W. Bange, S. Rapsomanikis, M. O. Andreae, *Global Biogeochem. Cycles* **10**, 197 (1996).
33. M. A. Altabet, M. J. Higginson, D. W. Murray, *Nature* **415**, 159 (2002).
34. A. Suthhof, V. Ittekkot, B. Gaye-Haake, *Global Biogeochem. Cycles* **15**, 637 (2001).
35. A. F. Bouwman, K. W. Van der Hoeck, J. G. J. Olivier, *J. Geophys. Res.* **100**, 2785 (1995).
36. C. S. Potter, P. A. Matson, P. M. Vitousek, E. A. Davidson, *J. Geophys. Res.* **101**, 1361 (1996).
37. C. S. Potter, S. A. Klooster, *Global Biogeochem. Cycles* **12**, 621 (1998).
38. E. A. Davidson, in *Microbial Production and Consumption of Greenhouse Gases: Methane, Nitrogen Oxides and Halomethanes*, J. E. Rogers, W. B. Whitman, Eds. (American Society for Microbiology, Washington, DC, 1991), pp. 219–235.
39. C. Kroeze, A. Mosier, L. Bouman, *Global Biogeochem. Cycles* **13**, 1 (1999).
40. C. Nevison, R. F. Weiss, D. J. I. Erickson, *J. Geophys. Res.* **100**, 15809 (1995).
41. J. E. Dore, B. N. Popp, D. M. Karl, F. J. Sansone, *Nature* **396**, 63 (1998).
42. K. Minschwaner, R. J. Salawitch, M. B. McElroy, *J. Geophys. Res.* **98**, 10543 (1993).
43. K. Minschwaner, R. W. Carver, B. P. Briegleb, A. E. Roche, *J. Geophys. Res.* **103**, 23243 (1998).
44. A. Berger, M. F. Loutre, *Quat. Sci. Rev.* **10**, 297 (1991).
45. P. M. Grootes, M. Stuiver, J. W. C. White, S. Johnsen, J. Jouzel, *Nature* **366**, 552 (1993).
46. J. M. Barnola, D. Raynaud, Y. S. Korotkevich, C. Lorius, *Nature* **329**, 408 (1987).

47. Supported by NSF–Office of Polar Programs (grants 9526556 to T.A.S. and 0087160 and 0126187 to R.B.A.). Special thanks to K. Keller, R. Najjar, J. Fluckiger, and two anonymous reviewers who greatly improved the manuscript.

Supporting Online Material
www.sciencemag.org/cgi/content/full/301/5635/945/DC1
SOM Text
Reference

3 April 2003; accepted 8 July 2003

340,000-Year Centennial-Scale Marine Record of Southern Hemisphere Climatic Oscillation

Katharina Pahnke,[1]* Rainer Zahn,[1,2]* Henry Elderfield,[3] Michael Schulz[4]

In order to investigate rapid climatic changes at mid-southern latitudes, we have developed centennial-scale paleoceanographic records from the southwest Pacific that enable detailed comparison with Antarctic ice core records. These records suggest close coupling of mid-southern latitudes with Antarctic climate during deglacial and interglacial periods. Glacial sections display higher variability than is seen in Antarctic ice cores, which implies climatic decoupling between mid- and high southern latitudes due to enhanced circum-Antarctic circulation. Structural and temporal similarity with the Greenland ice core record is evident in glacial sections and suggests a degree of interhemispheric synchroneity not predicted from bipolar ice core correlations.

Climatic instability and abrupt changes are recognized features of the last glacial period and have been found in climate archives worldwide (*1*–*6*). To date, the best-resolved records of changes in the Southern Hemisphere are from Antarctic ice cores (*5*, *6*). The dearth of continuous high-resolution paleoclimatic records from mid- and high southern latitudes precludes the tracing of climatic signals from Antarctic records to the extra-polar Southern Hemisphere. This highlights the importance of establishing fine-scale marine records that enable the mapping of millennial to submillennial climatic chang-

Downloaded from www.sciencemag.org on December 29, 2006